Neutrinos from SN 1987A, Earth matter effects, and the large mixing angle solution of the solar neutrino problem

C. Lunardini

SISSA-ISAS, via Beirut 2-4, 34100 Trieste, Italy
and INFN, sezione di Trieste, via Valerio 2, 34127 Trieste, Italy

A. Yu. Smirnov

The Abdus Salam ICTP, Strada Costiera 11, 34100 Trieste, Italy
and Institute for Nuclear Research, RAS, Moscow, Russia

We study the properties of the oscillation effects in the matter of the Earth on antineutrino fluxes from supernovae. We show that these effects can provide an explanation of the difference in the energy spectra of the events detected by Kamiokande-2 and IMB detectors from SN 1987A as well as the absence of high-energy events with $E \gtrsim 40$ MeV. This explanation requires the neutrino oscillation parameters Δm^2 and $\sin^2 2\theta$ to be in the region of the large mixing angle solution of the solar neutrino problem and the normal mass hierarchy if $|U_{e3}|^2 \gtrsim 10^{-3}$. The hierarchy can be inverted if $|U_{e3}|^2 \ll 10^{-3}$. The solution of the solar neutrino problem based on ν_e conversion to a pure sterile state is disfavored by SN 1987A data.

I. INTRODUCTION

The detection of the neutrino burst from SN 1987A by the Kamiokande-2 [1] and IMB [2] detectors has confirmed the general picture of gravitational collapse, hot neutron star formation, and neutrino emission (see [3,4] for a review).

At the same time certain features of the detected neutrino signals remain unexplained. In this paper we will consider the difference in the energy spectra of the events detected by Kamiokande-2 (K2) and IMB. It is difficult to explain such a difference in terms of the characteristics of the detectors (energy thresholds, efficiencies of detection, sizes, etc.). The $\bar{\nu}_e$ spectrum inferred from the K2 events is substantially softer than that from the IMB events. This can be quantified by comparing the parameters of the original $\bar{\nu}_e$ spectra, such as the effective temperature $T_{\bar{e}}$ and the luminosity $L_{\bar{e}}$ that were estimated from the results of the two experiments. It was found that the regions in the $T_{\bar{e}}$-$L_{\bar{e}}$ plane determined from the K2 and IMB data have only marginal overlap and the probability that the two sets of data correspond to the same spectrum is less than few percent [5].

More specifically, we will discuss the following features of the SN 1987A signals: (i) Concentration of the IMB events in the energy interval $E \simeq 35$–40 MeV; (ii) absence of events at IMB above $E \simeq 40$ MeV (which looks like a sharp cut of the spectrum); (iii) absence of events with $E \gtrsim 35$ MeV at K2.

The effects of mixing on supernova neutrinos have been extensively studied [6,7]. In particular, soon after the observation of SN 1987A it was noted that the differences in the K2 and IMB spectra could be related to oscillations of $\bar{\nu}_e$ in the matter of the Earth and to the different positions of the detectors at the time of detection [8,9]. It was realized that, for this oscillation mechanism to work, one needs $\Delta m^2 \sim 10^{-5}$ eV^2 (i.e., in the region of the Earth regeneration effect) and large (close to maximal) mixing of $\bar{\nu}_e$.

At that time the idea did not attract much attention, since a large lepton mixing was considered unnatural and conversion with small mixing angle was indicated as the most plausible solution of the solar neutrino problem. Moreover, later it was argued [10,11] that a large mixing of electron neutrinos is disfavored by the SN 1987A data: the $\bar{\nu}_e \leftrightarrow \bar{\nu}_\mu / \bar{\nu}_\tau$ conversion inside the star leads to the appearance of a high energy tail in the spectrum that contradicts observations. The bound is absent, however, in the range of Earth matter effects, $\Delta m^2 \sim 10^{-5}$ eV^2.

Later, the likelihood analysis of the combined K2 and IMB spectra in [12] has confirmed the results of [11]. In general, the flavor conversion of $\bar{\nu}_e$ leads to worse agreement with the supernova theory. Some mild improvement of the likelihood appears for oscillation parameters in the large mixing angle (LMA) region when the Earth matter effect is taken into account. This improvement is obtained, however, at the price of aggravating the conflict with the SN theory: it was found that the best fit point corresponds to too low a temperature of the original $\bar{\nu}_e$ spectrum, $T_{\bar{e}} \simeq 1.9$ MeV, and too high a total binding energy, $L \simeq 10^{54}$ ergs. Moreover, the best fit values $\Delta m^2 \simeq (3$–$5) \times 10^{-6}$ eV^2 found in [12] are now excluded by the Superkamiokande data on the day-night asymmetry.

Since the first proposal [8] the situation has drastically changed. With very high confidence level the atmospheric neutrino data are explained by $\nu_\mu \leftrightarrow \nu_\tau$ oscillations with maximal or nearly maximal mixing [13]. The LMA solution gives the best global fit of all the available solar neutrino data [14]. It seems that large mixing is a general property of leptons. Clearly, if the LMA is the true solution of the solar neutrino problem, then a significant part of the $\bar{\nu}_e$ events detected from SN 1987A were produced by the converted muon and tau antineutrinos. This means that in 1987 we observed the first appearance signal of neutrino conversion.

In view of this we have reconsidered the explanation of the features of the neutrino signals from SN 1987A in terms of neutrino conversion in the star and in the Earth.

In Sec. II we study the general properties of the conversion of antineutrinos in the matter of the supernova and of the Earth. We apply the results to the explanation of the difference of signals detected by Kamiokande-2 and IMB in Sec. III. In Sec. IV we summarize implications of the Earth matter effect on antineutrinos for the neutrino mass spectrum.

II. NEUTRINO CONVERSION IN THE STAR AND IN THE EARTH

We assume that the electron neutrino mixes with some combination of the muon and tau neutrinos, ν'_μ, ($\nu_e = \cos\theta\nu_1 + \sin\theta\nu_2$, $\nu'_\mu = \cos\theta\nu_2 - \sin\theta\nu_1$), and the oscillation parameters of the ν_e-ν'_μ system are in the region of the large mixing angle solution of the solar neutrino problem:

$$\sin^2 2\theta \simeq 0.6 - 1.0, \quad \Delta m^2 \simeq (1.5 - 10) \times 10^{-5} \text{ eV}^2, \quad (1)$$

[the case of LOW solution will be considered later]. We will also assume that other Δm^2 and mixings in the neutrino spectrum are irrelevant for the antineutrino channel.

With the parameters (1) the propagation of antineutrinos inside the star is completely adiabatic, so that the following transitions occur [15]:

$$\bar{\nu}_e \to \bar{\nu}_1, \quad \bar{\nu}'_\mu \to \bar{\nu}_2. \quad (2)$$

That is, the originally produced electron antineutrino will reach the surface of the star, and consequently the surface of the Earth, as the pure mass eigenstate $\bar{\nu}_1$, and $\bar{\nu}'_\mu$ as the pure mass eigenstate $\bar{\nu}_2$. As a result, the flux of the electron antineutrinos at the surface of the Earth equals

$$F_{\bar{e}} = \cos^2\theta F_{\bar{e}}^0 + \sin^2\theta F_{\bar{\mu}'}^0 = F_{\bar{e}}^0 - \sin^2\theta(F_{\bar{e}}^0 - F_{\bar{\mu}'}^0), \quad (3)$$

where $F_{\bar{e}}^0$ and $F_{\bar{\mu}'}^0$ are the original fluxes of $\bar{\nu}_e$ and $\bar{\nu}'_\mu$ produced in the center of the star.

In the matter of the Earth the mass eigenstates $\bar{\nu}_1$ and $\bar{\nu}_2$ oscillate. Taking into account these oscillations we find the flux of $\bar{\nu}_e$ at the detector [15]:

$$F_e^D = F_{\bar{e}} + (P_{1\bar{e}} - \cos^2\theta)(F_{\bar{e}}^0 - F_{\bar{\mu}'}^0), \quad (4)$$

where $P_{1\bar{e}}$ is the $\bar{\nu}_1 \to \bar{\nu}_e$ transition probability in the matter of the Earth; in the derivation of Eq. (4) we used also the relation $P_{2\bar{e}} = 1 - P_{1\bar{e}}$. Since for both K2 and IMB detectors the neutrino trajectories were in the mantle, where the density change is rather small, we use for $P_{1\bar{e}}$ the formula for oscillations in uniform medium [11]:

$$P_{1\bar{e}} = \cos^2\theta + \sin 2\theta_m \sin(2\theta - 2\theta_m)\sin^2\left(\frac{\pi d}{l_m}\right). \quad (5)$$

Here d is the length of the neutrino trajectory inside the Earth for a given detector, θ_m and l_m are the mixing angle and the oscillation length for the antineutrinos in the matter of the Earth:

$$\sin^2 2\theta_m = \frac{\sin^2 2\theta}{[\cos 2\theta + (l_\nu/l_0)]^2 + \sin^2 2\theta}, \quad l_m = l_\nu \frac{\sin 2\theta_m}{\sin 2\theta}. \quad (6)$$

In Eq. (6) $l_\nu \equiv 4\pi E/\Delta m^2$ and $l_0 \equiv 2\pi/(\sqrt{2}G_F n_e)$ are the vacuum oscillation length and the refraction length; G_F is the Fermi coupling constant and n_e is the electron number density. In expression (5) θ_m and l_m should be taken for the average electron number density n_e along the neutrino trajectory for a given detector.

The qualitative features of the conversion effects can be immediately seen from Eqs. (3)–(5), taking into account that the original $\bar{\nu}'_\mu$ flux has a harder spectrum than that of $\bar{\nu}_e$ and the total luminosities in the different flavors are comparable. This means that a critical energy, E_c, exists such that

$$F_{\bar{\mu}'}^0 > F_{\bar{e}}^0 \quad \text{for } E > E_c,$$

$$F_{\bar{\mu}'}^0 < F_{\bar{e}}^0 \quad \text{for } E < E_c. \quad (7)$$

The energy E_c depends, in particular, on the effective temperatures and luminosities of the original $\bar{\nu}'_\mu$ and $\bar{\nu}_e$ fluxes: $E_c = E_c(T_{\bar{e}}, T_{\bar{\mu}'}, L_{\bar{e}}, L_{\bar{\mu}'})$.

According to Eq. (3) the conversion in the star leads to a composite spectrum of electron antineutrinos with $\sin^2\theta$ admixture of the hard component, which generates an high energy tail in the sample of events. In comparison with the original $\bar{\nu}_e$ spectrum, $F_{\bar{e}}^0$, the flux $F_{\bar{e}}$ is suppressed at $E < E_c$ and enhanced at $E > E_c$. The effect is proportional to $\sin^2\theta$ and the conversion probability itself does not depend on the neutrino energy.

The oscillations inside the Earth give an opposite effect [see Eqs. (4) and (5)]: they enhance the flux at $E < E_c$ and suppress it at high energies. Notice that, since $P_{1\bar{e}} > \cos^2\theta$, for (LMA) parameters and in the constant density approximation the matter of the Earth always regenerates $\bar{\nu}_e$: the oscillatory factor in Eq. (5) is positive since $2\theta_m = (0-\pi)$ and $\theta > \theta_m$. Shortly, an increase of the medium density will tend to return the neutrino state into the initial state, that is, $\bar{\nu}_e$ at very high densities. Entering the Earth is equivalent to such an increase.

Combining Eqs. (3) and (4) we find

$$F_e^D = F_{\bar{e}}^0 - (F_{\bar{e}}^0 - F_{\bar{\mu}'}^0)(1 - P_{1\bar{e}}), \quad (8)$$

which shows that the overall conversion effect, both in the star and in the Earth, leads to suppression of the flux at low energies ($E < E_c$) and to its enhancement at high energies ($E > E_c$). The effect is proportional to the difference of the original fluxes.

Let us consider the properties of the Earth regeneration effect in some detail. Formula (8) can be written as

$$F_e^D = F_{\bar{e}}^0 - (F_{\bar{e}}^0 - F_{\bar{\mu}'}^0)(\sin^2\theta - A_p\sin^2\phi), \quad (9)$$

where

$$A_p \equiv \sin 2\theta_m \sin(2\theta - 2\theta_m), \quad \phi \equiv \frac{\pi d}{l_m} \quad (10)$$

are the depth and the phase of oscillations. In contrast to the conversion in the star, the Earth matter effect has strong energy dependence. The depth of oscillations, A_p, equals zero at very low energies, where $\theta_m \simeq \theta$, and at high energies, where $\theta_m \simeq \pi/2$. The depth reaches the maximum

$$A_p^{max} = \sin^2 \theta \quad (11)$$

at $\theta_m = \theta/2$, which corresponds to the equality

$$\frac{l_\nu}{l_0} = 1. \quad (12)$$

Notice that the depth of oscillations increases with θ. At the condition of maximal depth, Eq. (12), also the conversion probability $P_{1\bar{e}}$ reaches the maximum,

$$P_{1\bar{e}} = 1, \quad (13)$$

provided that $\phi = \pi/2 + k\pi$ with $k = 0,1,2, \ldots$. For $E \to 0$ or $E \to \infty$, we have $P_{1\bar{e}} \to \cos^2 \theta$. Thus, A_p as well as $P_{1\bar{e}}$ have a resonance character with Eq. (12) being the resonance condition. Notice that the condition (12) does not depend on the mixing angle, in contrast to the resonance condition for the pure flavor case.

From Eq. (12) we find the resonance energy

$$E_R = \frac{\Delta m^2}{2\sqrt{2}G_F n_e}. \quad (14)$$

The interval of energies $E_- - E_+$ around Eq. (14) for which $A_p > A_p^{max}/2 = \sin^2\theta/2$ is determined by

$$\frac{E_\pm}{E_R} = \cos 2\theta + 2 \pm \sqrt{(\cos 2\theta + 1)(\cos 2\theta + 3)}. \quad (15)$$

Thus E_R and $E_\pm$ give the interval of the strong oscillation effect in the Earth.

The peak in the $P_{1\bar{e}}$ probability exists in the antineutrino channel even if the usual flavor resonance is in the neutrino channel. With the increase of θ and its shift to the dark side, $\theta \gtrsim \pi/4$, the peak gets narrower and at $\theta \to \pi/2$ it converges to the usual flavor resonance peak. The oscillation length l_m decreases with $E/\Delta m^2$; it also decreases with $\cos 2\theta$.

At high energies, due to the exponential decrease of the fluxes with E and the difference of temperatures of the $\bar{\nu}_e$ and $\bar{\nu}'_\mu$ spectra, we get $F^0_{\mu'} \gg F^0_{\bar{e}}$, and therefore, according to Eq. (8), the flux at the detector equals

$$F^D_{\bar{e}} \simeq F^0_{\mu'}(1 - P_{1\bar{e}}). \quad (16)$$

Then, at resonance, $E \simeq E_R$, Eq. (14), the $\bar{\nu}_e$ flux can be suppressed completely: $F^D_{\bar{e}} \simeq 0$, if the phase of oscillations equals a semi-integer fraction of π. This suppression does not depend on the value of the mixing angle θ. In what

follows we will show that this suppression could indeed be realized in the case of neutrinos from SN 1987A.

III. NEUTRINO SIGNALS IN K2 AND IMB DETECTORS

Let us consider the difference of signals at K2 and IMB that can be produced by oscillations in the Earth. This difference is related to the distances travelled by the neutrinos in the Earth: $d_{IMB} \simeq 8535$ km for IMB, $d_{K2} \simeq 4363$ km for K2, and to the average densities $\rho_{IMB} \simeq 4.5$ g·cm^{-3}, $\rho_{K2} \simeq 3.5$ g·cm^{-3} along the trajectories. As a consequence, both the depths and the phases of oscillations at the K2 and IMB detectors are different.

Let us show that the features (i)–(iii) indicated in the Introduction can be explained by oscillations in the matter of the Earth. Moreover, the explanation implies certain values of Δm^2 and $\sin^2 2\theta$.

To reproduce the characteristics described in (i)–(iii) we require the following.

(1) The phase of oscillations at the IMB detector at $E \simeq 38$–42 MeV equals

$$\phi_{IMB}(40) \equiv \frac{\pi d_{IMB}}{l_m} = k\pi, \quad k = 1,2,3, \ldots . \quad (17)$$

Under this condition the oscillations in the matter of the Earth do not suppress the signal.

(2) The phase of oscillations at the IMB detector at $E \simeq 50$–60 MeV is a semi-integer of π:

$$\phi_{IMB}(60) = \pi\left(\frac{1}{2} + k\right), \quad k = 0,1,2, \ldots \quad (18)$$

so that in this range of energy one expects maximal suppression effect. It is easy to check that, in the range of parameters of interest, the conditions (17) and (18) are satisfied simultaneously with good precision.

(3) The phase of oscillations at the K2 detector at $E \simeq 38$–42 MeV is

$$\phi_{K2}(40) \equiv \frac{\pi d_{K2}}{l_m} = \pi\left(\frac{1}{2} + k\right), \quad k = 0,1,2, \ldots \quad (19)$$

so that the Earth matter effect produces maximal suppression of the K2 signal in the range $E \simeq 38$–42 MeV.

(4) The Earth matter effect is maximal, $A_p \simeq A_p^{max}$, at the IMB detector at the energies $E \simeq 50$–60 MeV, that is,

$$E_R^{IMB} \simeq 50 - 60 \text{ MeV}. \quad (20)$$

In Fig. 1 we show the conditions (17), (19), and (20) in the Δm^2-$\cos 2\theta$ plane. As follows from the figure, there are bands in which the requirements (17) and (19) are satisfied simultaneously. They correspond to $\phi_{IMB} \simeq 2\phi_{K2} = 3\pi, 5\pi, 7\pi, \ldots$. The phase increases with Δm^2. Notice that the requirements (17)–(19) are satisfied in the whole relevant range of $\cos 2\theta$ if ϕ_{IMB} equals odd multiples of π.

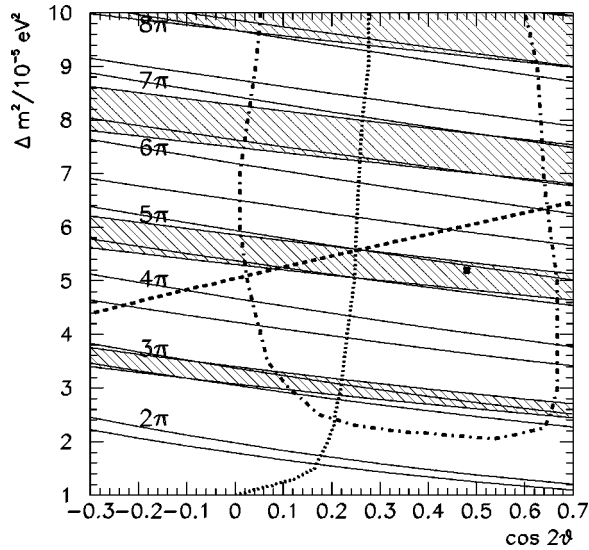The condition of maximal effect, Eq. (20), gives $\Delta m^2 = (1.7$–2.1)$\times 10^{-5}$ eV^2. A large Earth matter effect, e.g.,

FIG. 1. Bands of equal phases $\phi_{IMB}(40) = k\pi$ (dotted regions) and $\phi_{K2}(40) = \pi(1/2 + k)$ (dashed regions) in the Δm^2-$\cos 2\theta$ plane. The widths of the bands are determined by the requirement that the conditions (19) and (17) are satisfied in the energy interval $E = 38$–42 MeV. The region below the dashed line represents the band of strong Earth matter effect, where $A_p \gtrsim 0.7 A_p^{max}$ [see Eq. (20)]. For comparison we show the 99% C.L. allowed region of the LMA solution of the solar neutrino deficit (dotted-dashed contour, from [14]) where the best fit point is marked by an asterisk. The dotted line represents the 99% C.L. exclusion curve from Fig. 3a of Ref. [11].

$A_p \gtrsim 0.7 A_p^{max}$, is realized in a much wider interval, whose borders depend on $\cos 2\theta$ (the upper border is represented by the dashed line in Fig. 1).

As follows from Fig. 1 the explanation of the properties (i)–(iii) implies the oscillation parameters to be in the regions $\phi_{IMB} = 3\pi$ for all the relevant values of θ, and $\phi_{IMB} = 5\pi$ for $\cos 2\theta \gtrsim 0.2$. The central values of these bands are described, approximatively, by the following lines:

$$\Delta m^2 \simeq 3.3 \times 10^{-5} \text{ eV}^2 [1 - 0.35 \cos 2\theta],$$

$$\Delta m^2 \simeq 5.6 \times 10^{-5} \text{ eV}^2 [1 - 0.18 \cos 2\theta]. \tag{21}$$

For $\cos 2\theta \gtrsim 0.1$ the values (21) are well inside the 99% confidence limit (CL) allowed region of the LMA solution (dotted-dashed contour in Fig. 1, from Ref. [14]). Moreover, the best-fit point, $\cos 2\theta \simeq 0.5$, $\Delta m^2 \simeq 5.2 \times 10^{-5}$ eV^2,[1] lies in the band $\phi_{IMB} \simeq 5\pi$ [see Eq. (21)].

Figure 1 shows also the 99% C.L. exclusion curve obtained in Ref. [11] (dotted line), corresponding to the upper bound on the permutation parameter $p = 0.35$. One can see that the region $\cos 2\theta \lesssim 0.25$ is excluded; this region was ob-

tained taking $T_{\bar{e}} \simeq 4.5$ MeV and $T_{\bar{\mu}'} \simeq 7.4$ MeV; it becomes narrower for the lower values of the temperatures we consider in this paper.

The expected distributions of events are rather sensitive to variations of Δm^2. For instance, a change of Δm^2 by $\sim 20\%$ in the $\phi_{IMB} = 3\pi$ band will lead to the prediction of strong suppression of the number of events in the interval $E \simeq 35$–40 MeV of the IMB spectrum and enhancement of the signal at $E \simeq 50$ MeV, in contradiction with observations.

Let us consider the expected spectra of events at the K2 and IMB detectors. The original instantaneous $\bar{\nu}_e$ and $\bar{\nu}_{\mu'}$ fluxes can be described by "pinched" Fermi-Dirac spectra with pinching parameter $\eta \simeq 2$ [16]. However, once integrated over arrival time intervals Δt of several seconds, the spectra are well approximated by the ordinary Fermi-Dirac form, i.e., with $\eta = 0$, as an effect of the decay with time of the neutrino luminosities and temperatures. This description is good if Δt is not larger than the typical decay time τ of the temperatures and luminosities. For $\Delta t \gtrsim \tau$ the integrated spectra cannot be approximated by a Fermi-Dirac form. This is the case of the SN 1987A data, which show a rapid cooling of the neutrino spectra with decay time comparable or smaller than the duration of the burst, $\tau \lesssim \Delta t_b \simeq 13$ s. Therefore, we have divided the whole time interval of observations in two bins, $t_1 = 0$–6.5 s and $t_2 = 6.5$–13 s, and described the integrated fluxes over each bin by Fermi-Dirac spectra with different temperatures $[T(t_1) > T(t_2)]$ and luminosities $[L(t_1) > L(t_2)]$. We note that the values of T and L we give should be considered as effective (time averaged) quantities.

In Figs. 2 and 3 we show the expected spectra of events at the K2 and IMB detectors in the first time bin ($t < 6.5$ s) for two sets of parameters from the preferable regions, Eq. (21). They have been obtained taking $T_{\bar{e}} = 3.5$ MeV, $T_{\bar{\mu}'} = 7$ MeV and $\eta_{\bar{\mu}'} = \eta_{\bar{e}} = 0$. We assumed equal integrated luminosities in $\bar{\nu}_e$ and $\bar{\nu}_{\mu'}$: $L_{\bar{e}} = L_{\bar{\mu}'} = 3 \times 10^{52}$ ergs. The energy thresholds and detection efficiencies have been taken into account.

According to the figures, the predicted spectra with oscillations (solid lines) fit the observed distributions of events at K2 and IMB detectors better. As expected, the spectra without oscillations (dashed lines) cannot describe the concentration of IMB events at $E \simeq 30$–40 MeV and the absence of an excess of K2 events in this range. The conversion in the star only leads to an appearance of high energy tails (short dashed lines) that contradict the observations of both K2 and IMB detectors. The oscillations in the matter of the Earth (solid lines) suppress the tails above 45 MeV in IMB and above 35 MeV in K2.[2] Notice that the figures have an illustrative character and do not correspond to the optimal (best fitted) choice of parameters of the original spectra.

To quantify the improvement of the fit due to conversion inside the star and the Earth matter effect we have performed

---

[1] This result is given by the global two-neutrino fit of the solar neutrino data including the total rates and the day and night spectra at the Super-Kamiokande detector [14].

[2] Notice that in our analysis the maximal suppression, due to oscillations in the Earth, of the antineutrino signal in IMB occurs at energies above 50 MeV. For such energies the efficiency of the IMB detector was high ($\mathcal{E}_{IMB} \gtrsim 0.7$).
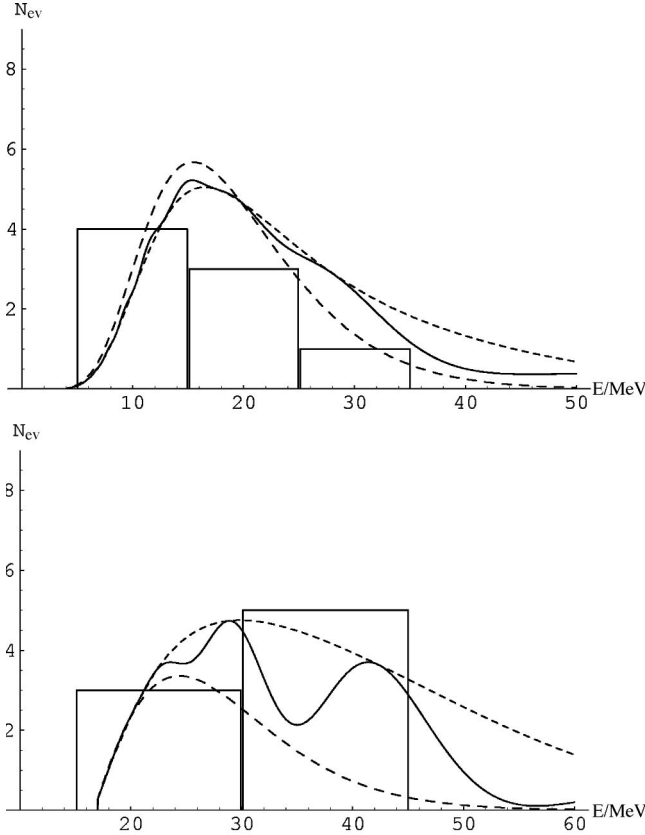
FIG. 2. The predicted spectra of $\bar{\nu}_e$ events at the Kamiokande-2 (upper panel) and IMB (lower panel detectors). We show the original spectra without oscillation effects (long dashed lines), spectra with conversion in the star only (dashed lines), spectra with oscillation effects both in the star and in the Earth (solid lines). We used the following set of oscillation parameters and characteristics of the original $\bar{\nu}_e$ and $\bar{\nu}'_\mu$ spectra: $T_{\bar{e}}=3.5$ MeV, $L_{\bar{e}}=3\times10^{52}$ ergs, $\eta_{\bar{e}}=0$, $T_{\bar{\mu}'}=7$ MeV, $L_{\bar{\mu}'}=3\times10^{52}$ ergs, $\eta_{\bar{\mu}'}=0$, $\cos 2\theta=0.5$, $\Delta m^2=2.75\times10^{-5}$ eV^2. The histograms show the observed distributions of events during the first 6.5 s.

the likelihood analysis following, in general, the prescriptions of Ref. [12]. There are, however, some differences.

(1) We have divided the whole energy range of the detected events into several bins. The size ΔE of each bin has been chosen according to the experimental errors ϵ in the measurements of energy: $\Delta E \sim 2\epsilon$. We used three bins with $\Delta E = 10$ MeV for K2 and two bins with $\Delta E = 15$ MeV for IMB (see histograms in the Figs. 2 and 3).

(2) We computed the realization probability P of a given theoretical prediction using the Poissonian distribution:

$$P = \prod_i \frac{(n_i)^{N_i}}{N_i!} e^{-n_i}, \qquad (22)$$

where N_i is the number of observed events in the ith bin and $n_i = n_i(T_{\bar{e}}, T_{\bar{\mu}'}, L_{\bar{e}}, L_{\bar{\mu}'}, \Delta m^2, \theta)$ is the corresponding number of expected events that depends on the parameters of the original neutrino spectra and oscillation parameters. We find the maximum of P and the contours of given confidence levels according to Ref. [12].
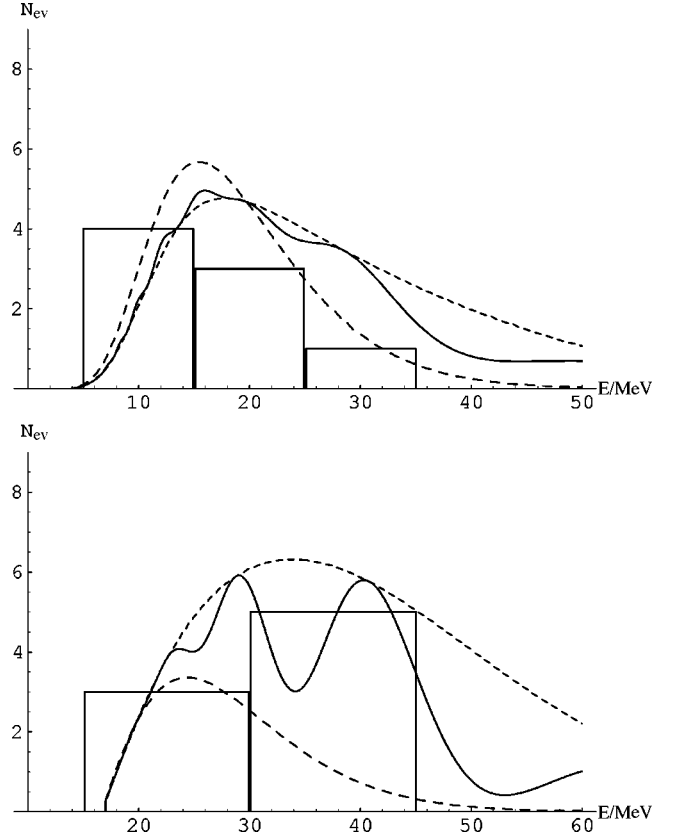
FIG. 3. The same as Fig. 2 with $\cos 2\theta=0.2$, $\Delta m^2=3\times10^{-5}$ eV^2.

Notice that, in contrast with [12] we use a discrete (binned) expression of the probability P and we calculate n_i by integrating the corresponding predicted function $n(E)$ over the ith energy bin. By this procedure we take into account the experimental errors on energies with no need to introduce any energy resolution function as it is done in [12].

(3) We performed separate analyses of the K2 and IMB data collected in the two time bins t_1 and t_2; no events are discarded in this procedure.[3]

In Fig. 4 we show the results of the likelihood analysis of the IMB and K2 data of the first time bin in the $T_{\bar{e}}$-$L_{\bar{e}}$ plane in absence of mixing, $\theta=0$ (upper panel). As follows from the figure, K2 and IMB spectra imply substantially different temperatures of the original $\bar{\nu}_e$ spectrum: $T_{K2}\simeq2.8$ MeV and $T_{IMB}\simeq4.2$ MeV. There is no overlap of the 68% CL regions.

The lower panel of Fig. 4 shows the analogous plot in presence of oscillations in the star and in the matter of the Earth. We have taken $T_{\bar{\mu}'}/T_{\bar{e}}=1.8$, $L_{\bar{\mu}'}/L_{\bar{e}}=1$, $\eta_{\bar{e}}=\eta_{\bar{\mu}'}=0$ with oscillation parameters from the preferable bands (see Fig. 1). With oscillations the best fit parameters inferred from IMB and K2 data become closer: $T_{K2}\simeq1.96$ MeV and $T_{IMB}\simeq2.75$ MeV. We get $\Delta T/T \equiv 2(T_{IMB}-T_{K2})/(T_{IMB}+T_{K2})\simeq0.33$ and 0.41 with and without oscillations respec-

---

[3]The event number 6 in the K2 data has been considered as due to background, following Ref. [12]; however our conclusions remain unchanged when this event is considered.
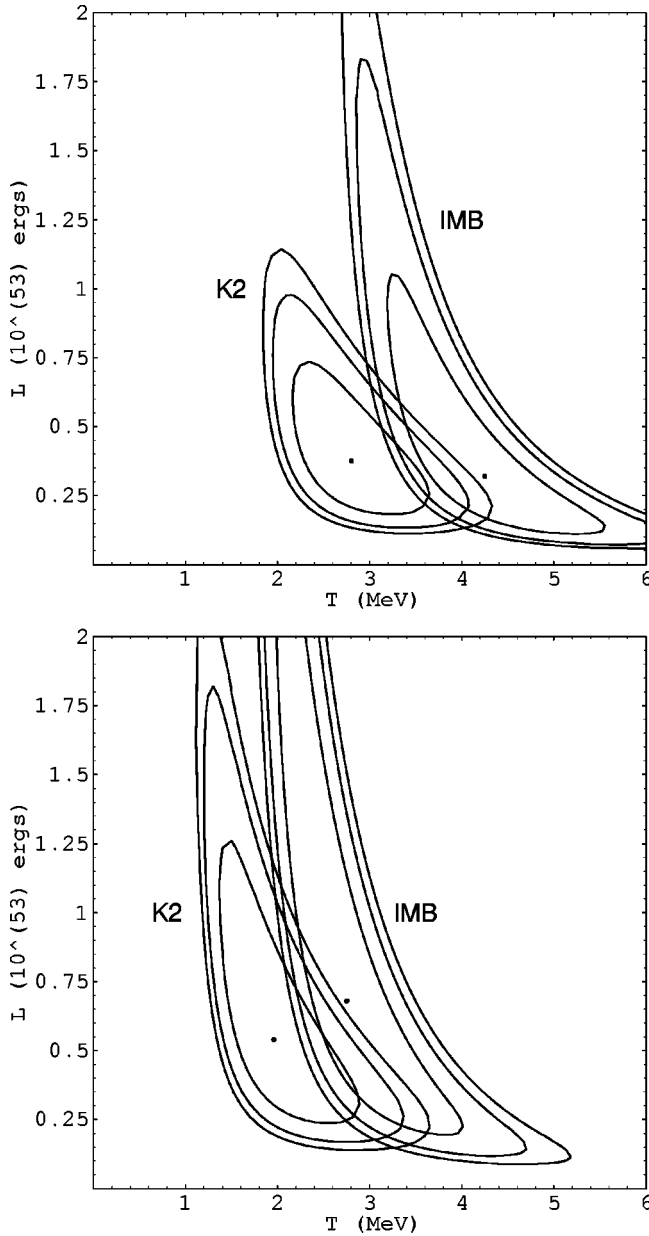
FIG. 4. Best fit points and contours of equal 68, 90, 95.4 % likelihood for K2 and IMB detectors in the $T_{\bar{e}}$-$L_{\bar{e}}$ plane. The upper panel shows the result of the separate fits of K2 and IMB data without oscillation effects. The lower panel represents a similar fit in presence of oscillations. The following values for the oscillation parameters and characteristics of original spectra have been used: $T_{\bar{\mu}'}/T_{\bar{e}}=1.8$, $L_{\bar{\mu}'}/L_{\bar{e}}=1$, $\eta_{\bar{e}}=\eta_{\bar{\mu}'}=0$ and $\cos 2\theta=0.2$, $\Delta m^2=3 \times 10^{-5}$ eV^2.

tively. Overlap of the 68% CL regions appears. The combined fit gives $T_{\bar{e}}\simeq 2.77$ MeV and $L_{\bar{e}}\simeq 4.4\times 10^{52}$ ergs, which are in good agreement with recent calculations [17]. Thus, the likelihood analysis with oscillations shows some improvement of the fit and does not imply too low temperatures and high luminosities.

In the second time bin K2 has detected 3 events with low energies, close to the threshold, whereas IMB has no signals. This can be easily interpreted in the assumption of lower

temperatures of the $\bar{\nu}_e$ and $\bar{\nu}_{\mu'}$ original spectra and smaller difference of $T_{\bar{\mu}'}$ and $T_{\bar{e}}$. Taking for instance $T_{\bar{e}}\simeq T_{\bar{\mu}'} \simeq 1.8$ MeV and $L_{\bar{e}}\simeq L_{\bar{\mu}'}\simeq 3\times 10^{52}$ ergs we predict ~ 2 events in K2 with energy $E\simeq 5-15$ MeV and less than 0.5 events at $E\geqslant 15$ MeV. With the same values of the parameters we get less than 0.2 events in the IMB spectrum, that is, with high probability all the events are below the IMB threshold.

For neutrino parameters from the LOW solution, $\Delta m^2 =(0.3-2)\times 10^{-7}$ eV^2, $\sin^2 2\theta\gtrsim 0.95$, we get $l_0/l_\nu \lesssim 10^{-2}$, so that the mixing angle in matter is suppressed: $\sin 2\theta_m \simeq \sin 2\theta(l_0/l_\nu)$. For the depth of oscillations in the Earth matter we find from Eq. (10):

$$A_p \simeq \sin^2 2\theta\left(\frac{l_0}{l_\nu}\right), \qquad (23)$$

that is, $A_p\ll 1$. Thus, the effect of oscillations in the Earth is negligibly small. Now $P_{1\bar{e}}\simeq\cos^2\theta$ and the $\bar{\nu}_e$ flux at Earth is determined by the conversion inside the star only [see Eq. (3) and the short dashed lines in the Figs. 2 and 3]. No improvement of the fit can be obtained in this case.

IV. IMPLICATIONS FOR THE NEUTRINO MASS SPECTRUM

The fact of observation of the Earth matter effect in the $\bar{\nu}_e$ channel by itself has important implications for the neutrino mass spectrum and mixing (see also [15]).

(1) As we have shown, a significant effect is possible for oscillation parameters in the LMA region only: thus, the observation of the effect selects the LMA solution of the solar neutrino problem. In the cases of small mixing angle (SMA) or LOW solutions the Earth matter effect would be practically unobservable.

(2) Important conclusions can be drawn on the type of mass hierarchy and the mixing element U_{e3} in the three neutrino context. Let us consider the three neutrino scheme that explains also the atmospheric neutrino problem via $\nu_\mu\leftrightarrow\nu_\tau$ oscillations. In this scheme the third mass eigenstate, ν_3, is isolated from ν_1 and ν_2, which are responsible for the solar neutrino oscillations, by the mass gap $\Delta m^2_{23}\simeq\Delta m^2_{atm}\simeq 3 \times 10^{-3}$ eV^2. The state ν_3 has nearly a maximal mixture of ν_μ and ν_τ. The admixture of the ν_e in this state, described by the matrix element $|U_{e3}|^2$, is small being restricted by the reactor experiments CHOOZ [18] and Palo Verde [19]: $|U_{e3}|^2\lesssim 0.02-0.05$.

Observation of the matter effect means that (i) either the mass hierarchy is normal, $\Delta m^2_{23}=m^2_3-m^2_2>0$ (the third state is the heaviest one) or, (ii) if the hierarchy is inverted, $\Delta m^2_{23}<0$, the ν_e-ν_3 mixing is very small: $|U_{e3}|^2\ll 10^{-3}$.

Indeed, in the first case the high density resonance associated with Δm^2_{23} ($\rho_R\sim\Delta m^2_{23}$) is in the neutrino channel. It does not influence the conversion of antineutrinos and the situation coincides with the one considered above.

If, however, the hierarchy is inverted the high density resonance is in the antineutrino channel. The pattern of conversion then strongly depends on the adiabaticity in this reso-

nance. If $|U_{e3}|^2 \gtrsim 10^{-3}$ the level crossing is adiabatic, so that in the star the conversions

$$\bar{\nu}_e \rightarrow \bar{\nu}'_\tau, \quad \bar{\nu}'_\tau \rightarrow \bar{\nu}'_\mu/\bar{\nu}_e, \quad \text{and} \quad \bar{\nu}'_\mu \rightarrow \bar{\nu}'_\mu/\bar{\nu}_e \qquad (24)$$

occur. Thus, the $\bar{\nu}_e$ flux at Earth will be composed of converted $\bar{\nu}'_\mu$ and $\bar{\nu}'_\tau$ fluxes. Since the original $\bar{\nu}'_\mu$ and $\bar{\nu}'_\tau$ fluxes are identical, no matter effect should be seen in the $\bar{\nu}_e$ flux [15,20]. Moreover, the $\bar{\nu}_e$ flux will have the hard spectrum of the original $\bar{\nu}'_\mu$ and $\bar{\nu}'_\tau$ fluxes, which is disfavored by observations [11].

If $|U_{e3}|^2 \ll 10^{-3}$, the adiabaticity in the high density resonance is broken. The effect of this resonance can be neglected and the pattern of the three neutrino conversion is reduced to the two neutrino case discussed in the paper.

If $|U_{e3}|^2 \simeq 10^{-5}-10^{-3}$, one can observe an intermediate situation: harder $\bar{\nu}_e$ spectrum and partially suppressed Earth matter effect.

If $|U_{e3}|^2 \gtrsim 10^{-3}$ (which looks rather plausible in view of the large mixing between the first and the second as well as the second and the third generations) we come to the conclusion that the observation of the Earth matter effect in the $\bar{\nu}_e$ channel implies a scheme with normal mass hierarchy and the LMA solution of the solar neutrino problem.

(3) Let us consider the Earth matter effect for supernova neutrinos in the case of ν_e-ν_s mixing. As for active neutrinos, for ν_e-ν_s a significant effect is possible for large mixing angles (notice, however, that large mixing $\nu_e \rightarrow \nu_s$ conversion gives poor fit of the solar neutrino data).

We assume that no sterile antineutrino fluxes are generated in the central part of the star.[4] In this case we get the result for the $\bar{\nu}_e$ flux at the detector from Eq. (8) setting $F^0_{\mu'} = 0$:

$$F^D_e = P^s_{1e} F^0_e. \qquad (25)$$

Here P^s_{1e} is the probability of $\bar{\nu}_1 \rightarrow \bar{\nu}_e$ oscillations in the matter of the Earth for mixing with sterile neutrino.

The difference of potentials for the ν_e-ν_s system, $V_{es} = \sqrt{2} G_F (n_e - n_n/2) \simeq V_{e\mu}/2$, is about two times smaller than the one of the ν_e and ν_μ species, $V_{e\mu}$. In the last equality we considered that the medium is almost isotopically neutral in the mantle of the Earth. Correspondingly, the refraction length is two times larger than in the active-active case, so that, according to Eq. (12) the range of large matter effects is shifted to smaller Δm^2 by a factor 2.

From Eq. (25) we see that, in contrast with ν_e-ν'_μ mixing, the observed events in the detector are due to the original $\bar{\nu}_e$ flux only, and no hard tail appears in the spectrum. As a consequence, no improvement in the fit of K2 and IMB data

is obtained with respect to the $\theta = 0$ case. Moreover, it is possible to check that a larger $\bar{\nu}_e$ luminosity is required.

The discussion of Secs. II and III can be immediately generalized to the case in which the electron neutrino is mixed with both an active neutrino ν_μ and a sterile one, ν_s. The problem can be reduced to ν_e-ν_x mixing, with $\nu_x = \sqrt{1-\delta}\nu_\mu + \sqrt{\delta}\nu_s$; the pure active and pure sterile mixings correspond to $\delta = 0$ and $\delta = 1$, respectively. Now the $\bar{\nu}_e$ flux in the detector is given by Eq. (8) with $F^0_x = (1-\delta)F^0_{\mu'}$. Thus, with respect to the pure active case, one gets a reduction by a factor $\sim(1-\delta)$ of the hard part of the detected spectrum. For $\delta \lesssim 0.5$ still one gets a good fit of the K2 and IMB signals.

V. CONCLUSIONS

We have studied properties of the oscillation effects in the matter of the Earth on neutrino signals from supernovae. We show that certain features of the neutrino signal from SN 1987A detected by K2 and IMB detectors (difference of spectra, absence of events above $E \sim 40$ MeV) can be explained by oscillations in the Earth and different positions of the detectors. The consistency of the $\bar{\nu}_e$ spectra implied by K2 and IMB data improves when oscillations are taken into account.

The existence of the Earth matter effects on the neutrino burst from supernovae has crucial implications for the neutrino mass spectrum.

(1) The oscillation parameters Δm^2 and $\sin^2 2\theta$ should be in the range of the LMA solution of the solar neutrino problem. Moreover, the values of Δm^2 and $\sin^2 2\theta$ should lie in rather narrow bands.

(2) The mass hierarchy (in the three neutrino context) should be normal, if $|U_{e3}|^2 \gtrsim 10^{-3}$ and it can be inverted provided that $|U_{e3}|^2 \ll 10^{-3}$.

It should be stressed that, in view of the low statistics of SN 1987A neutrino signals, our conclusions have an indicative character, as far as the interpretation of the K2 and IMB data is concerned. If the LMA solution will be identified in future experiments, the inclusion of the effects of oscillations in the matter of the Earth in the analysis of SN 1987A data will be unavoidable, and the interpretation of SN 1987A signals given in this paper will be confirmed. The analysis performed in this paper shows that searches for oscillation effects in the matter of the Earth in future observations of galactic supernovae will give important information on the neutrino mass spectrum, independently of supernova models.

Note added. In the recent paper [21] a new analysis of the SN 1987A signal is performed, based on the Kolmogorov test of the K2 data only, with the conclusion that the LMA solution of the solar neutrino problem is excluded at high confidence level. However the Earth matter effect, which we have shown here to be crucial, is not taken into account.

---

[4]A sterile state ν_s can be produced, however, by conversion of active neutrinos at high densities in the star. This happens in some schemes with four neutrinos, which explain the Liquid Scintillation Neutrino Detector (LSND) result.

[1] KAMIOKANDE-II Collaboration, K. Hirata *et al.*, Phys. Rev. Lett. **58**, 1490 (1987).

[2] R. M. Bionta *et al.*, Phys. Rev. Lett. **58**, 1494 (1987).

[3] H. Suzuki, in *Physics and Astrophysics of Neutrinos*, edited by M. Fukugita and A. Suzuki (Springer Verlag, Berlin, 1994).

[4] G. G. Raffelt, *Stars as Laboratories for Fundamental Physics: The Astrophysics of Neutrinos, Axions, and Other Weakly Interacting Particles* (University of Chicago Press, Chicago, 1996).

[5] For analyses of K2 and IMB signals see, e.g., L. M. Krauss, Nature (London) **329**, 689 (1987); A. Burrows, Astrophys. J. **334**, 891 (1988); H. T. Janka and W. Hillebrandt, Astron. Astrophys. **224**, 49 (1989); see also [4] for a discussion.

[6] S. P. Mikheev and A. Y. Smirnov, Zh. Éksp. Teor. Fiz. **91**, 7 (1986) [Sov. Phys. JETP **64**, 4 (1986)].

[7] Neutrino conversion in collapsing stars is discussed also in D. Notzold, Phys. Lett. B **196**, 315 (1987); J. Arafune, M. Fukugita, T. Yanagida, and M. Yoshimura, *ibid.* **194**, 477 (1987); T. P. Walker and D. N. Schramm, *ibid.* **195**, 331 (1987); T. K. Kuo and J. Pantaleone, Phys. Rev. D **37**, 298 (1988); H. Minakata and H. Nunokawa, *ibid.* **38**, 3605 (1988); P. J. Kernan and L. M. Krauss, Nucl. Phys. **B437**, 243 (1995); G. Dutta, D. Indumathi, M. V. Murthy, and G. Rajasekaran, Phys. Rev. D **62**, 093014 (2000); G. Dutta, D. Indumathi, M. V. Murthy, and G. Rajasekaran, *ibid.* **61**, 013009 (2000).

[8] A. Y. Smirnov, talk given at the Twentieth International Cosmic Ray Conference, Moscow, 1987.

[9] The Earth matter effects on the electron neutrino flux from neutronization have been discussed in J. Arafune, M. Fukugita, T. Yanagida, and M. Yoshimura, Phys. Rev. Lett. **59**, 1864 (1987); H. Minakata, H. Nunokawa, K. Shiraishi, and H. Suzuki, Mod. Phys. Lett. A **2**, 827 (1987).

[10] L. Wolfenstein, Phys. Lett. B **194**, 197 (1987).

[11] A. Y. Smirnov, D. N. Spergel, and J. N. Bahcall, Phys. Rev. D **49**, 1389 (1994).

[12] B. Jegerlehner, F. Neubig, and G. Raffelt, Phys. Rev. D **54**, 1194 (1996).

[13] Super-Kamiokande Collaboration, Y. Fukuda *et al.*, Phys. Rev. Lett. **81**, 1562 (1998).

[14] See, e.g., G. L. Fogli, E. Lisi, D. Montanino, and A. Palazzo, Phys. Rev. D **62**, 113003 (2000); M. C. Gonzalez-Garcia and C. Peña-Garay, hep-ph/0009041.

[15] A. S. Dighe and A. Y. Smirnov, Phys. Rev. D **62**, 033007 (2000).

[16] H. T. Janka and W. Hillebrandt, Astron. Astrophys. **224**, 49 (1989).

[17] A. Burrows, T. Young, P. Pinto, R. Eastman, and T. Thompson, astro-ph/9905132. For earlier calculations see A. Burrows, Astrophys. J. **334**, 891 (1988); Janka and Hillebrandt [16]; H. T. Janka and W. Hillebrandt, Astron. Astrophys. **224**, 49 (1989); E. S. Myra and A. Burrows, Astrophys. J. **364**, 222 (1990); A. Burrows, D. Klein, and R. Gandhi, Phys. Rev. D **45**, 3361 (1992); S. Yamada, H. Janka, and H. Suzuki, astro-ph/9809009.

[18] CHOOZ Collaboration, M. Apollonio *et al.*, Phys. Lett. B **466**, 415 (1999); **420**, 397 (1998).

[19] Palo Verde Collaboration, F. Boehm *et al.*, Phys. Rev. D **62**, 072002 (2000).

[20] See also H. Minakata, talk given at NOW2000, Otranto, Italy, 2000, http://www.ba.infn.it/now2000

[21] D. B. Cline, astro-ph/0010339.